Molecular Cell, Volume *63*

Supplemental Information

Molecular Basis of Assembly and Activation of Complement Component C1 in Complex with Immunoglobulin G1 and Antigen

Guanbo Wang, Rob N. de Jong, Ewald T.J. van den Bremer, Frank J. Beurskens, Aran F. Labrijn, Deniz Ugurlar, Piet Gros, Janine Schuurman, Paul W.H.I. Parren, and Albert J.R. Heck

Figure S1

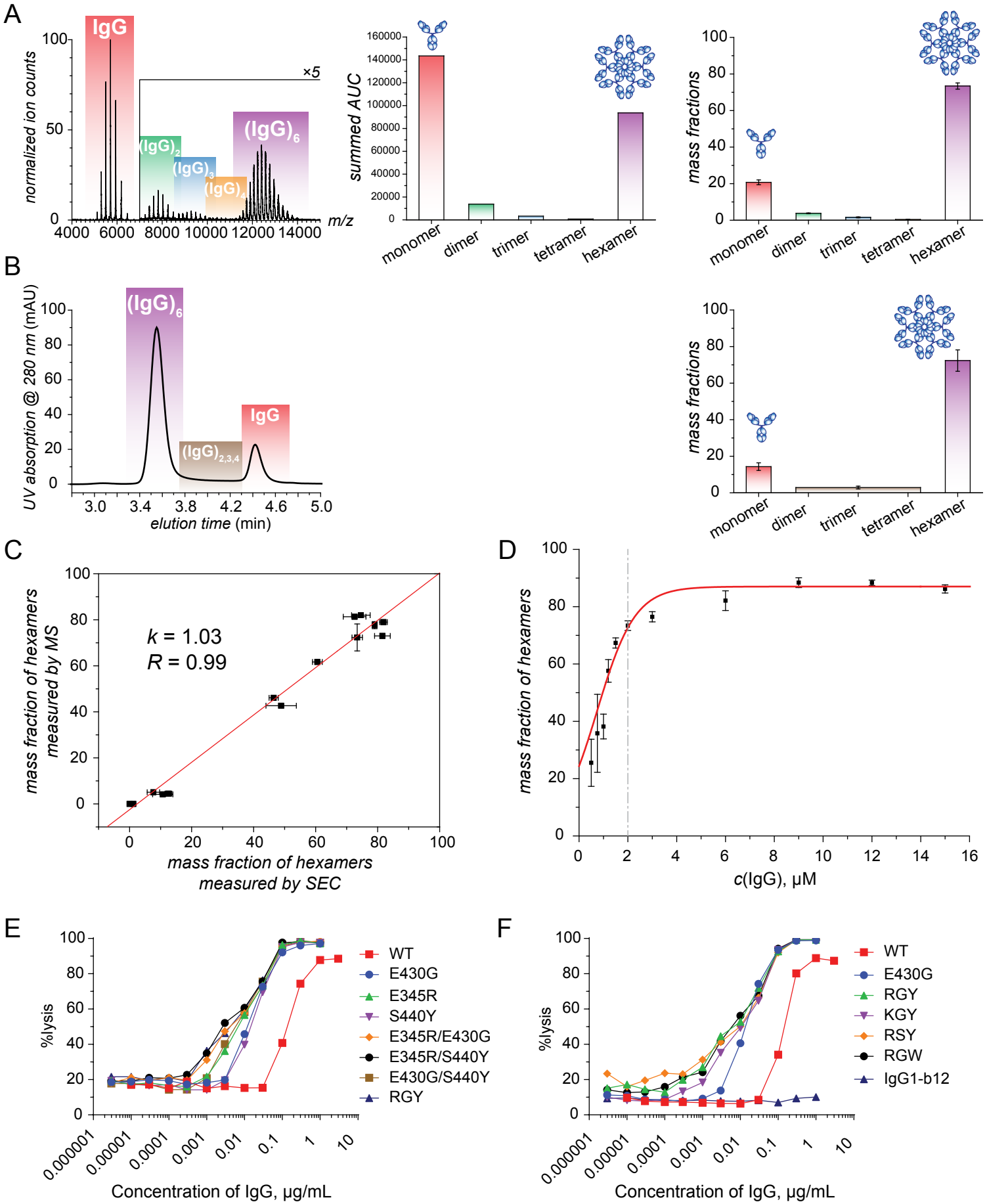
A
IgG
×5
(IgG)2
(IgG)3
(IgG)4
(IgG)6
normalized ion counts
m/z
summed AUC
monomer
dimer
trimer
tetramer
hexamer
mass fractions
B
(IgG)6
IgG
(IgG)2,3,4
UV absorption @ 280 nm (mAU)
elution time (min)
C
k = 1.03
R = 0.99
mass fraction of hexamers measured by MS
mass fraction of hexamers measured by SEC
D
mass fraction of hexamers
c(IgG), µM
E
%lysis
WT
E430G
E345R
S440Y
E345R/E430G
E345R/S440Y
E430G/S440Y
RGY
Concentration of IgG, µg/mL
F
WT
E430G
RGY
KGY
RSY
RGW
IgG1-b12

Figure S2

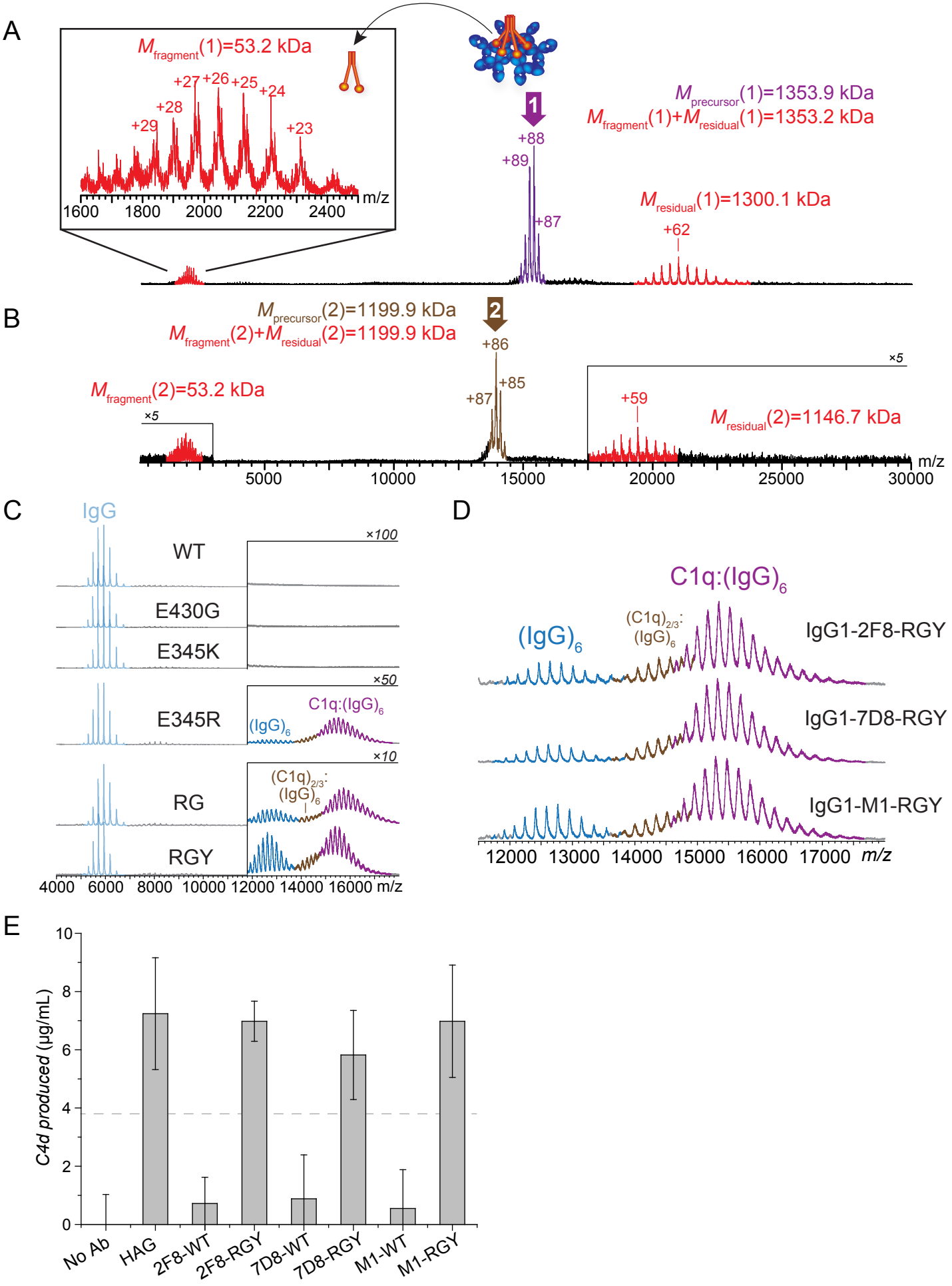
A
$M_{fragment}$(1)=53.2 kDa
+27 +26 +25 +24
+28
+29
+23
1600 1800 2000 2200 2400 m/z
$M_{precursor}$(1)=1353.9 kDa
$M_{fragment}$(1)+$M_{residual}$(1)=1353.2 kDa
+88
+89
+87
$M_{residual}$(1)=1300.1 kDa
+62
B
$M_{precursor}$(2)=1199.9 kDa
$M_{fragment}$(2)+$M_{residual}$(2)=1199.9 kDa
+86
+85
+87
×5
$M_{fragment}$(2)=53.2 kDa
×5
+59
$M_{residual}$(2)=1146.7 kDa
5000 10000 15000 20000 25000 30000 m/z
C
IgG
WT
E430G
E345K
E345R
RG
RGY
×100
×50
×10
C1q:(IgG)$_6$
(IgG)$_6$
(C1q)$_{2/3}$:(IgG)$_6$
4000 6000 8000 10000 12000 14000 16000 m/z
D
C1q:(IgG)$_6$
(IgG)$_6$
(C1q)$_{2/3}$:(IgG)$_6$
IgG1-2F8-RGY
IgG1-7D8-RGY
IgG1-M1-RGY
12000 13000 14000 15000 16000 17000 m/z
E
C4d produced (µg/mL)
0 2 4 6 8 10
No Ab
HAG
2F8-WT
2F8-RGY
7D8-WT
7D8-RGY
M1-WT
M1-RGY

Figure S3

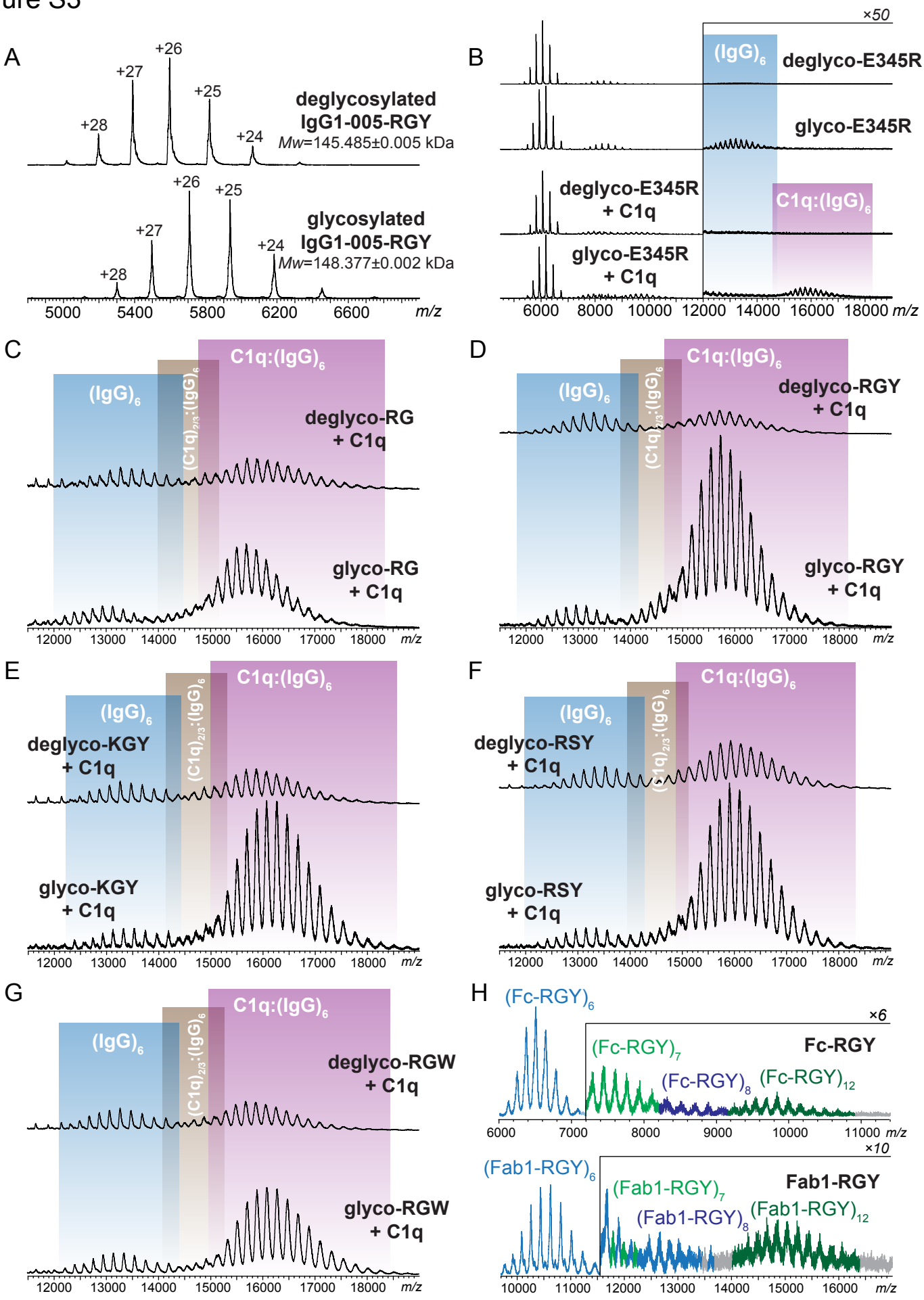
A
deglycosylated
IgG1-005-RGY
Mw=145.485±0.005 kDa
glycosylated
IgG1-005-RGY
Mw=148.377±0.002 kDa
+28
+27
+26
+25
+24
5000
5400
5800
6200
6600
m/z
B
×50
(IgG)6
deglyco-E345R
glyco-E345R
deglyco-E345R
+ C1q
glyco-E345R
+ C1q
C1q:(IgG)6
6000
8000
10000
12000
14000
16000
18000
m/z
C
(IgG)6
C1q:(IgG)6
(C1q)2/3:(IgG)6
deglyco-RG
+ C1q
glyco-RG
+ C1q
12000
13000
14000
15000
16000
17000
18000
m/z
D
(IgG)6
C1q:(IgG)6
(C1q)2/3:(IgG)6
deglyco-RGY
+ C1q
glyco-RGY
+ C1q
E
(IgG)6
C1q:(IgG)6
(C1q)2/3:(IgG)6
deglyco-KGY
+ C1q
glyco-KGY
+ C1q
F
(IgG)6
C1q:(IgG)6
(C1q)2/3:(IgG)6
deglyco-RSY
+ C1q
glyco-RSY
+ C1q
G
(IgG)6
C1q:(IgG)6
(C1q)2/3:(IgG)6
deglyco-RGW
+ C1q
glyco-RGW
+ C1q
H
(Fc-RGY)6
(Fc-RGY)7
(Fc-RGY)8
(Fc-RGY)12
×6
Fc-RGY
6000
7000
8000
9000
10000
11000
m/z
(Fab1-RGY)6
(Fab1-RGY)7
(Fab1-RGY)8
(Fab1-RGY)12
×10
Fab1-RGY
10000
11000
12000
13000
14000
15000
16000
m/z

Figure S4

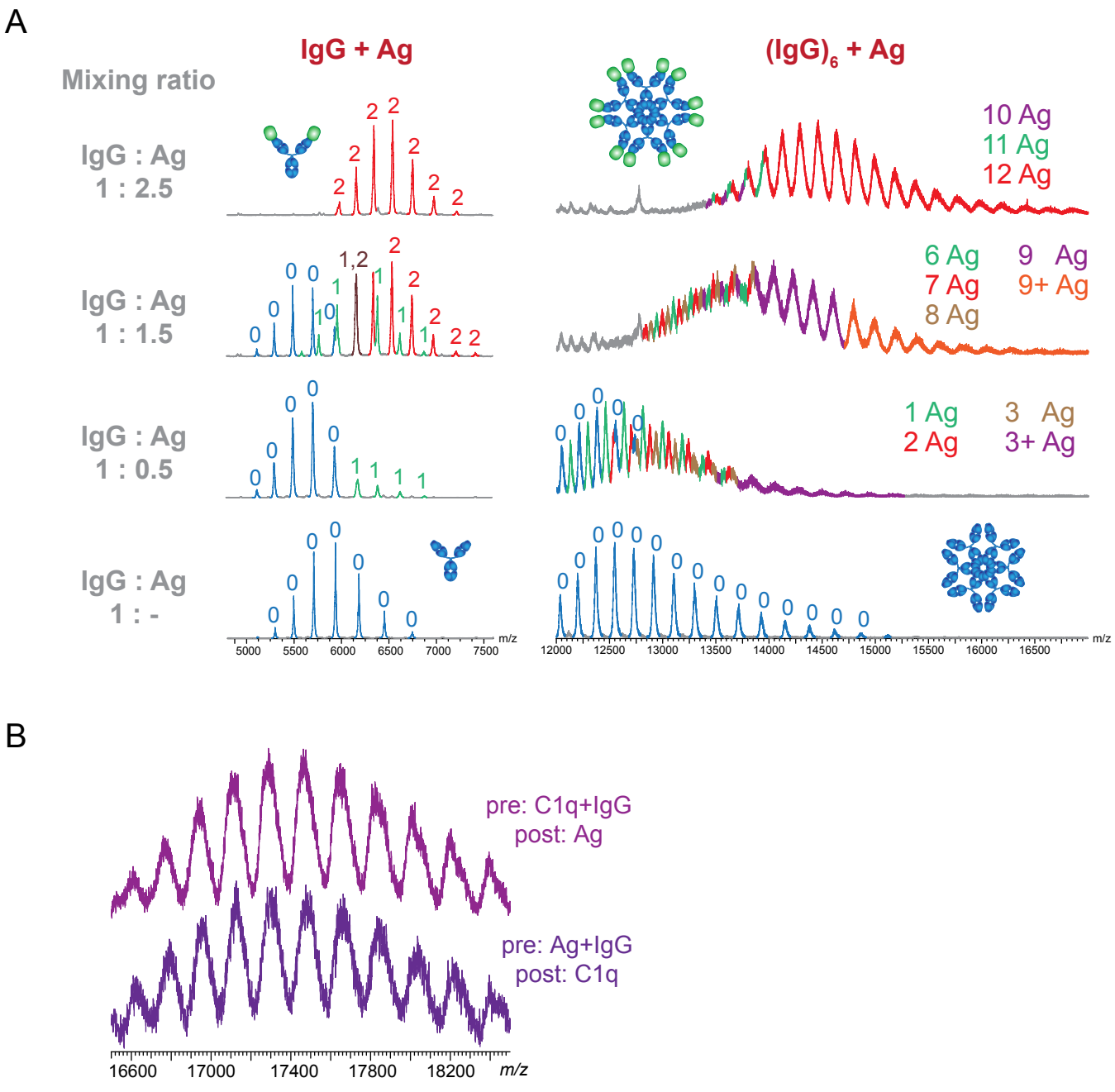
A
IgG + Ag
(IgG)6 + Ag
Mixing ratio
IgG : Ag
1 : 2.5
IgG : Ag
1 : 1.5
IgG : Ag
1 : 0.5
IgG : Ag
1 : -
10 Ag
11 Ag
12 Ag
6 Ag
7 Ag
8 Ag
9 Ag
9+ Ag
1 Ag
2 Ag
3 Ag
3+ Ag
m/z
5000
5500
6000
6500
7000
7500
12000
12500
13000
13500
14000
14500
15000
15500
16000
16500
B
pre: C1q+IgG
post: Ag
pre: Ag+IgG
post: C1q
16600
17000
17400
17800
18200
m/z

Figure S5

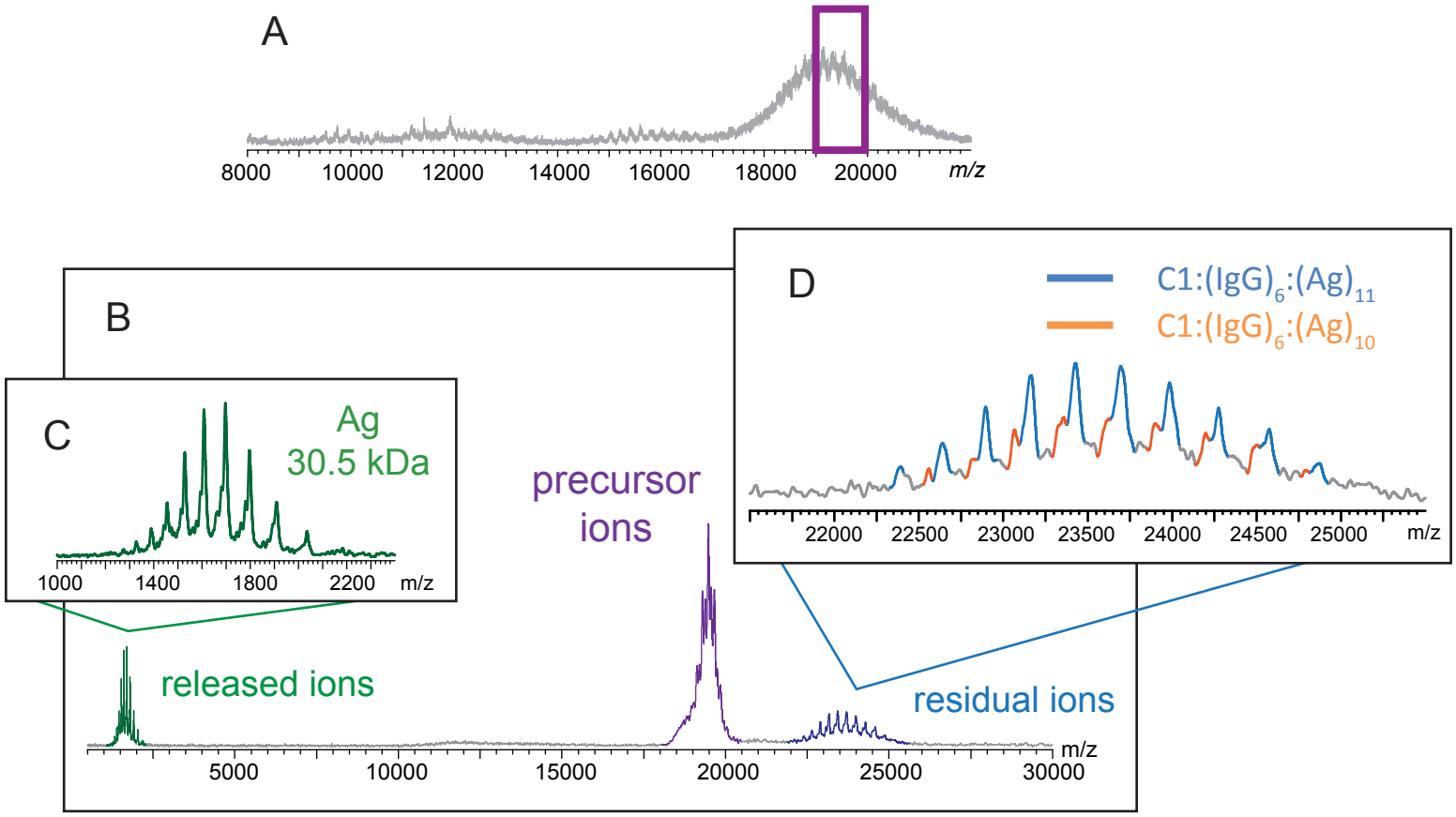
A
8000
10000
12000
14000
16000
18000
20000
m/z
B
C
Ag
30.5 kDa
1000
1400
1800
2200
m/z
D
C1:(IgG)6:(Ag)11
C1:(IgG)6:(Ag)10
22000
22500
23000
23500
24000
24500
25000
m/z
precursor
ions
released ions
residual ions
5000
10000
15000
20000
25000
30000
m/z

Supplemental Figure Legends

Figure S1. **Native MS and SEC measurements result in highly consistent quantitation of hexameric IgG variants. (Related to Figure 1)**

(A) Quantitation of protein complexes from ion count data. The total ion count of a given species is integrated from the raw spectrum (left), followed by integration of the total ion count of a given species, which is plotted to present the molar distribution of the corresponding species (middle). Afterwards the vertical axis is converted to the mass fraction scale (right) by multiplication of the molar abundance of a complex with the number of incorporated IgG subunits (followed by normalization), to present the percentage of IgG molecules incorporated in each oligomeric state.

(B) Quantitation of the mass fractions extracted from the UV absorbance data following SEC. Low abundant oligomers of intermediate size could not be resolved using this method.

(C) Comparison of hexameric IgG abundance quantitated by SEC (x-axis) and native MS (y-axis).

(D) Relative abundance of IgG hexamer as a function of the monomer concentration of IgG1-005-RGY. Data were fitted with a dose-response curve. The vertical dashed line indicates the default IgG concentration used throughout this work.

(E) CDC of Ramos cells opsonized with IgG1-005 wild type or variant antibodies containing mutations E345R, E430G and S440Y or combinations thereof.

(F) Ramos cells opsonized with IgG1-005 wild type, IgG1-005 containing a single E430G mutation or triple mutants mutated at E345R, E430G and S440Y (RGY) and variants thereof carrying the E345K, E430S or S440W mutation.

The graphs with error bars in (A-D) represent the average ± standard deviation ($n \geq 3$).

Figure S2. **Hexameric IgG variants bind C1q and activate complement in solution. (Related to Figure 2)**

(A-B) Accurate Mw determination of C1q:IgG complexes reveals that IgG1-005-RGY binds C1q in the hexameric state. Subpopulations of ions indicated by the arrows in Figure 2B were mass-selected for subsequent collision induced dissociation (CID), which resulted in release of a disulfide linked hetero-dimer of C1q A-B chains with high charge-density, and the corresponding residuals with low charge-density. The resulting tandem MS spectra of species labeled as 1 and 2 are shown in Panel (A) and (B), respectively, where charge states are labeled on top of the representative peaks. The accurate Mw determination of selected precursor ions is consistent with the summed Mw of released fragments and

corresponding residuals. The Mw of Species 1 agrees with the theoretical Mw of C1q:$(IgG)_6$ (Table S2). The Mw difference between Species 1 and 2 is approximately 154 kDa, in agreement with the Mw of 1/3 C1q ($A_2B_2C_2$), *i.e.* 154.5 kDa, indicating that Species 2 is assembled from 2/3 C1q and 6 copies of IgG. This assignment is consistent with the presence of 2/3 C1q signals prior to the incubation of C1q with IgG (Figure 2B, bottom panel). Since the Mw of monomeric IgG1-005-RGY is 148.1 kDa, the observed signals do not support the formation of C1q:$(IgG)_5$.

(C) Native MS analysis of C1q binding to $(IgG)_6$ variants.

(D) Efficient C1q binding was observed by native MS for multiple IgG1-RGY Abs directed against distinct antigens. Signal peaks representing $(IgG)_6$, $(C1q)_{2/3}$:$(IgG)_6$ and C1q:$(IgG)_6$ are colored in blue, brown and purple, respectively.

(E) C4d ELISA of IgG1-005 mutants detecting solution-phase complement activation in serum. The baseline is defined as twice the standard deviation for control measurements. HAG is a preparation of polyclonal heat aggregated human IgG. Data are presented as average ± standard deviation (n=3).

Figure S3. Deglycosylation and removal of Fab-arms affect hexamerization and C1q-binding of IgG. (Related to Figure 3)

(A) Comparison of native mass spectra of IgG1-005-RGY before and after deglycosylation, indicating the complete removal of glycan chains.

(B-G) Deglycosylation of detectably hexamerizing IgG variants decreases C1q-binding efficiency. Native MS characterization of C1q binding to glycosylated and deglycosylated $(IgG)_6$ variants. In Panel B intensities of the signals with *m/z* higher than 12000 were magnified by 50 for better visualization of $(IgG)_6$ and C1q:$(IgG)_6$; in Panel C-G signals were normalized based on the intensities of $(IgG)_6$ signals to illustrate the relative extent of C1q:$(IgG)_6$ formation. Signals of $(IgG)_6$, $(C1q)_{2/3}$:$(IgG)_6$ and C1q:$(IgG)_6$ are shaded in blue, brown and purple, respectively.

(H) Removal of Fab-arms enables supra-hexameric oligomerization**.** Native MS analysis of IgG1-RGY variants lacking either one (Fab1-RGY) or both Fab-arms (Fc-RGY) demonstrates the formation of hexamers, and of low-abundance heptamers, octamers and dodecamers. Signal intensities were amplified 6-fold (for Fc-RGY) or 10-fold (for Fab1-RGY) to visualize the less-abundant species.

Figure S4. **Saturating, bivalent antigen binding by IgG does not interfere with hexamerization or C1q recruitment. (Related to Figure 4)**

(A) Native MS analysis of antigen (Ag) CD38-ECD titrated into a solution of anti-CD38 Ab IgG1-005-RGY. Depending on the amount of Ag, each IgG monomer bound 0-2 Ags and each $(IgG)_6$ bound 0-12 Ags. Unambiguous determination of binding stoichiometries was achieved by following a previously described procedure (Dyachenko et al., 2015).

(B) Pre-incubation of C1q and IgG followed by incubation with excess Ag or pre-incubation of IgG and excess Ag followed by incubation with C1q, resulted in the same MS pattern and binding stoichiometry of the C1q:IgG:Ag complex.

Figure S5. **C1, Ab and Ag assemble into complexes with a 1:6:12 stoichiometry. (Related to Figure 5)**

During tandem MS analysis, ions of the intact C1:Ab:Ag complex were mass-selected (selection window illustrated by a purple box overlaid to Panel A, an MS1 spectrum) and subjected to collision-induced dissociation (Panel B; signals representing precursor ions shown in purple), which resulted in release of 1 Ag molecule with high charge-density (green trace in Panel B; a zoom-in view shown in Panel C). The residual part of the complexes with lower charge-density gave rise to signals with better spectral resolution (orange and blue traces in Panel B; a zoom-in view shown in Panel D), allowing their corresponding masses to be determined unambiguously. The predominant residual species is identified as $C1:(IgG)_6:(Ag)_{11}$, suggesting that prior to the dissociation the stoichiometry of predominant intact complex was C1:Ab:Ag = 1:6:12.

Supplemental Tables

Table S1. Mutations present in all the IgG variants used in this work and the corresponding abbreviations. Amino acids were numbered according to EU-nomenclature (Kabat, 1991). (Related to Figure 1-4)

Abbreviation	Full Name	mutation sites
HAG	Heat-aggregated IgG	N/A
WT	IgG1-005-WT	N/A
N297Q	IgG1-005-N297Q	N297Q
E345R	IgG1-005-E345R	E345R
E345K	IgG1-005-E345K	E345K
E430G	IgG1-005-E430G	E430G
S440Y	IgG1-005-S440Y	S440Y
RG	IgG1-005-RG	E345R/E430G
RY	IgG1-005-RY	E345R/S440Y
GY	IgG1-005-GY	E430G/S440Y
RGY	IgG1-005-RGY	E345R/E430G/S440Y
KGY	IgG1-005-KGY	E345K/E430G/S440Y
RSY	IgG1-005-RSY	E345R/E430S/S440Y
RGW	IgG1-005-RGW	E345R/E430G/S440W
RGK	IgG1-005-RGK	E345R/E430G/S440K
2F8-WT	IgG1-2F8-WT	N/A
2F8-RGY	IgG1-2F8-RGY	E345R/E430G/S440Y
7D8-RGY	IgG1-7D8-RGY	E345R/E430G/S440Y
M1-RGY	IgG1-M1-RGY	E345R/E430G/S440Y
Fc-RGY	Recombinant Fc fragment of IgG1-RGY	E345R/E430G/S440Y
Fab1-RGY	Asymmetric antibody molecule generated using DuoBody technology (Labrijn et al., 2014) comprised of an IgG-F405L and an Fc-K409R arm, both containing RGY mutations [a].	E345R/F405L/E430G/S440Y (for IgG1-005), and E345R/K409R/E430G/S440Y (for Fc)

[a] See ***Experimental Procedures*** for detail.

Table S2. Theoretical and measured Mw values of the proteins or protein complexes used or identified in this work. (Related to Figure 1-5)

		Theoretical MW [a] (kDa)	Measured MW [b] (kDa)	Number of charge states used for calculation
proteins	IgG1-005-WT	145.370 + *M*(g)	148.059±0.004	6
	IgG1-005-RGY	145.432 + *M*(g)	148.377±0.002	6
	IgG1-005-RGY (deglycosylated)	145.432	145.485±0.005	6
	Fc-RGY	50.039 + *M*(g)	53.013±0.006	4
	Fab1-RGY	97.729 + *M*(g)	100.730±0.005	6
	CD38-ECD (deglycosylated)	30.473	30.484±0.001	4
	C1q	421.149 + *M*(g)	464.13±0.04	9
	C1r-S654A	78.197 + *M*(g)	84.618±0.005	4
	C1s-S632A	74.871 + *M*(g)	78.524±0.009	5
protein complexes [c]	$(IgG)_2$	296.75	296.76±0.02	7
	$(IgG)_3$	445.13	445.06±0.01	7
	$(IgG)_4$	593.51	593.43±0.04	7
	$(IgG)_6$	890.26	890.20±0.03	12
	$(IgG)_6$ (deglycosylated)	872.9	873.0±0.2	11
	$(Fc\text{-}RGY)_6$	318.08	318.21±0.04	6
	$(Fab1\text{-}RGY)_6$	604.4	604.8±0.1	8
	$(IgG)_1:(Ag)_2$	209.345	*209.294±0.009*	6
	$(IgG)_6:(Ag)_{12}$	1255.9	*1255.2±0.1*	9
	$C1q:(Fc\text{-}RGY)_6$	782.3	782.6±0.3	9
	$C1q:(Fab1\text{-}RGY)_6$	1068.9	*1068.2±0.2*	7
	$C1q:(IgG)_6$	1354.4	*1353.2±0.2*	6
	$C1q:(IgG)_6:(Ag)_{12}$	1720.0	*1719.6±0.1*	9
	C1	790.4	*790.3±0.1*	6
	$C1:(IgG)_6$	1680.5	*1679.5±0.4*	8
	$C1:(IgG)_6:(Ag)_{12}$	2046.3	*2045.3±0.4*	9

[a] For proteins, calculated based on amino acid sequence, excluding contribution from glycan chains or other post-translational modification or processing (e.g., N-terminal K-processing for IgG); for protein complexes, calculated based on the measured Mw of the subunits. *M*(g) denotes Mw of Glycan contents.

[b] Including the contribution from glycan chains (for the glycosylated form only) and other post-translational modification or processing; tabulated are Mw of the most abundant forms. Values in Italic style represent results from tandem MS measurements.

[c] In IDs of these exemplary protein complexes "IgG" denotes IgG1-005-RGY and "Ag" denotes non-glycosylated CD38-ECD.

Table S3. Mass fraction of hexameric species measured for various IgG variants. (Related to Figure 1 and 3)

IgG ID	mass fraction of hexamer, %	standard deviation, % (n≥3)
WT	0	0
E345R	1.2	0.4
E345R (deglycosylated)	0	0
E345K	0	0
E430G	0	0
S440Y	0	0
RG	8	2
RG (deglycosylated)	0.8	0.2
RY	13	1
GY	11	3
RGY	73	2
RGY (saturated with CD38-ECD)	72	4
RGY (deglycosylated)	45	2
KGY	61	2
KGY (deglycosylated)	27	6
RSY	75	3
RSY (deglycosylated)	66	6
RGW	49	5
RGW (deglycosylated)	10	5
RGK	0	0
2F8-RGY	82	3
7D8-RGY	73	4
M1-RGY	79	1
Fc-RGY	51	5
Fab1-RGY	50	6

Table S4. Theoretical and measured Mw values of the proteins or protein complexes which were assembled at suboptimal stoichiometries presented in the Figures of the main text. (Related to Figure 2, 3 and 5)

	Theoretical MW [a] (kDa)	Measured MW [b] (kDa)	Number of charge states used for calculation	Related Figure
$(C1q)_{2/3}$	309.4	309.04±0.02	8	2B
$(C1q)_{2/3}$:$(IgG)_6$ [c]	1199.6	*1199.9±0.2*	6	2B
$(C1q)_{2/3}$:$(Fc\text{-}RGY)_6$	627.62	627.03±0.07	6	3E
$(C1q)_{2/3}$:$(Fab1\text{-}RGY)_6$	913.6	*913.5±0.1*	4	3E
C1q:C1r:C1s	627.3	627.2±0.7	6	5A
C1q:C1r:C1s:$(IgG)_6$	1517.5	*1517.2±0.4*	4	5A

[a] Calculated based on the measured Mw of the subunits tabulated in Table S2.

[b] Values in Italic style represent results from tandem MS measurements.

[c] "IgG" denotes IgG1-005-RGY.

Supplemental References

DYACHENKO, A., WANG, G. B., BELOV, M., MAKAROV, A., DE JONG, R. N., VAN DEN BREMER, E. T. J., PARREN, P. & HECK, A. J. R. (2015). Tandem Native Mass-Spectrometry on Antibody-Drug Conjugates and Submillion Da Antibody-Antigen Protein Assemblies on an Orbitrap EMR Equipped with a High-Mass Quadrupole Mass Selector. Anal. Chem. *87***,** 6095-6102.

KABAT, E. A. (1991). *Sequences of proteins of immunological interest,* Bethesda, MD, U.S. Dept. of Health and Human Services, Public Health Service, National Institutes of Health.

LABRIJN, A. F., MEESTERS, J. I., PRIEM, P., DE JONG, R. N., VAN DEN BREMER, E. T. J., VAN KAMPEN, M. D., GERRITSEN, A. F., SCHUURMAN, J. & PARREN, P. (2014). Controlled Fab-arm exchange for the generation of stable bispecific IgG1. Nat. Protoc. *9***,** 2450-2463.